ICSBM 2025
4th International Conference of Sustainable Building Materials
10-13 August, Eindhoven The Netherlands
G. Kaur, J. M. Fernández, I. Navarro-Blasco, S. Pavia, J I Álvarez (2025) From Toxic Waste to Sustainable Building: Red mud Cementitious Composites for Environmental Remediation
Proceedings ICSBM 2025 : 4th International Conference on Sustainable Building Materials: Volume 4 : Traditional and New Cementitious Materials ISBN 978-90-386-6618-1

From Toxic Waste to Sustainable Building: Red mud Cementitious Composites for Environmental Remediation

Gurbir Kaur[1], José María Fernández[1], Íñigo Navarro-Blasco[1], Sara Pavia[2], José Ignacio Álvarez[1]

[1]MATCH Research Group, Department of Chemistry, School of Sciences, University of Navarra, C/. Irunlarrea 1, 31008 Pamplona, Spain

[2]Trinity College Dublin, Ireland, The University of Dublin, College Green, Dublin 2, Ireland

Abstract

This study evaluates mortar containing up to 15% red mud as a cement substitute, focusing on strength, pore structure, and hydration behaviour. The primary goal of this study is to evaluate red mud as a low-cost and effective photocatalyst for air pollutant degradation. Further the study briefly examines the photocatalytic performance of red mud-based composites coated with titanium dioxide (TiO_2) to assess whether the incorporation of red mud affects the visible light absorption characteristics of TiO_2.

The findings suggest that incinerating red mud at 600ºC does not improve the pozzolanic activity of red mud. The low reactivity and lack of desirable compounds in red mud affect both strength development and pore refinement in cementitious materials, leading to decreased compressive strength and increased porosity in red mud-based mortars. Increasing red mud content led to significant strength loss, with oven-dried red mud-based samples i.e., R10-105 and R15-105 showing 20% and 44% reductions in compressive strength, while incinerated red mud-based counterparts exhibited a 20–31% decrease compared to the control. Nevertheless, incorporation of red mud into cementitious mortars yields materials with high photocatalytic efficiency for nitrogen oxides removal, achieving Class 3 performance in air purification level with over 8% NO degradation. Incorporating red mud alters the visible light absorption of TiO_2, with the TiO_2-coated R5-105-F-CI sample achieving a 26% higher NO removal under visible light compared to R5-105-F-CO. It is attributed to synergistic effects and enhanced charge separation at the Fe_2O_3/TiO_2 interface, underscoring the potential of red mud–TiO_2 composites for effective pollutant degradation.

Incorporating red mud into cementitious materials enables the development of multifunctional building products that support both structural and environmental functions. Particularly suitable for non-structural applications like red mud-based tiles, this approach aligns with sustainable construction by promoting circular economy principles and offering potential for environmental remediation through photocatalytic properties.

Keywords: photocatalytic activity, NO abatement, red mud, cementitious mortars, engineering properties

1 Introduction

The Bayer process is the main industrial method for refining bauxite into alumina, the key material for aluminium production. This process generates a highly alkaline waste called red mud or bauxite residue, with approximately 1 to 1.5 tonnes produced per tonne of alumina. Due to its high pH (10–12.5), red mud poses serious environmental risks, including soil and water contamination [1-2]. Global metallurgical alumina production is likely to increase from 124 million tonnes in 2019 to 178 million tonnes by 2040 [3]. Red mud contains valuable metals such as iron, titanium, and aluminium, with iron being the most abundant—mainly present as hematite, goethite, and ilmenite. This high iron content makes red mud a promising resource for iron recovery. Although laboratory and pilot-scale processes have achieved iron recovery rates of 70% to 96% [4], these results have not yet translated to large-scale industrial recycling.

Currently, only about 3% of the red mud generated annually is recycled, predominantly in the construction sector following costly neutralization processes. Researchers have explored the incorporation of red mud into various materials, including cement, ceramics, bricks, geopolymers, and asphalt [5-7]. Partial replacement of cement with red mud can reduce both environmental impact and CO_2 emissions; however, its use in mortar and concrete is typically restricted to a maximum of 15% by weight. Higher substitution levels tend to compromise mechanical properties such as strength and durability, primarily due to inadequate hydration and increased water demand [8]. According to the literature, thermal activation of red mud at temperatures between 600 and 800 °C enhances its reactivity, making it a more effective partial cement substitute—generally within the 5–30% replacement range [9]. Incinerating red mud at 600°C has significant pozzolanic activity, forming hydration products such as C–S–H and ettringite [10]. Nevertheless, the properties of red mud can vary significantly depending on its source, necessitating individual evaluation of each sample for suitability [11].

Red mud, rich in iron oxides such as hematite, has shown promise as a solar-active photocatalyst for pollutant degradation due to its narrow band gap (2.0–2.2 eV), allowing visible light absorption up to 600 nm. Modified red mud composites, such as those doped with cobalt or combined with materials like bagasse or graphitic carbon nitride, have demonstrated high photocatalytic performance and reusability under sunlight [12-14]. These findings underscore the potential of red mud-derived materials as sustainable, low-cost photocatalysts for environmental applications. In contrast, TiO_2, though widely used, requires UV activation due to its wide band gap. Efforts to improve its visible-light responsiveness focus on band gap engineering techniques such as doping, coupling, and defect modification, making it a key area of interest for solar-driven environmental remediation.

In light of these developments, integrating red mud with photocatalysts such as TiO_2 presents a promising dual-functional approach that addresses both waste valorisation and environmental remediation. By tailoring the optical and structural properties of red mud-based composites, particularly through synergistic coupling with semiconductors, it is possible to enhance visible-light-driven photocatalytic performance while utilizing red mud as a low-cost, sustainable resource.

Therefore, the aim of this study is twofold: first, to evaluate the effects of incorporating oven-dried and thermally activated red mud (incinerated at 600°C) as partial cement replacements on the engineering properties of cementitious mortars, including compressive strength, flexural strength, pore structure, and hydration behaviour; and second, to investigate the photocatalytic potential of red mud-based mortars for nitric oxide (NO) removal under visible light. The study also explores the synergistic effects of combining red mud with TiO_2 coatings, particularly focusing on how red mud influences the visible light absorption and photocatalytic efficiency of TiO_2. By integrating red mud into both the cementitious matrix and photocatalytic surface layers, this research seeks to assess the feasibility of red mud as a dual-function material for sustainable construction and environmental remediation.

2 Experimental programme

2.1 Materials and methods

Mortars were prepared using CEM III/A 42.5 N/SRC cement and siliceous standard sand. Red mud obtained from Alcoa San Ciprian in Lugo, Spain, was incorporated as a partial cement substitute up to 15% by weight. The chemical composition of binders i.e., cement, red mud oven dried at 105°C for 24 hours (RM-OD) and red mud incinerated at 600°C for 3 hours (RM-I), is presented in Table1 (values obtained through XRF). A standard 1:3 cement-sand by weight mortar with 0.5 water-cement ratio served as a control mix. Six different mixtures were prepared by substituting cement with either RM-OD or RM-I at 5%, 10%, and 15% by weight. Specimens were cast to assess the compressive and flexural strength after curing periods of 7 and 28 days. The specimens were maintained at a temperature of 20°C and a relative humidity exceeding 95% until they reached their specified testing ages.

The isothermal calorimetry test data in terms of heat flow and cumulative heat during the initial 72 hours of hydration was monitored using a TAM AIR isothermal microcalorimeter set to a constant temperature of 25°C. Approximately 10 g of paste mixture was prepared and promptly placed into an ampoule, which was then swiftly inserted into the calorimeter for measurement.

Mercury intrusion porosimetry was employed to analyse the pore structure of mortars. The examination was conducted using a Micromeritics AutoPore IV 9500 device, applying pressures ranging from 0.0015 to 207 MPa on regular mortar fragments.

The nitric oxide (NO) abatement test is performed on red mud-based mortar samples both with and without TiO_2 coating to systematically evaluate the photocatalytic properties of these materials. In this test, the degradation rate of NO gas is measured under controlled conditions which involve exposing the mortar samples to a flow of NO gas and quantifying the reduction in NO concentration due to photocatalytic reactions on the sample surface. The photoreactor is fed by a 0.78 L min−1 flow of NO and air with an initial NO concentration of 500 ppb. After a 30-minute equilibration period to account for surface adsorption, samples undergo a one-hour illumination using a 300 W Ultravitalux lamp. A glass longpass filter with a 420 nm cut-on wavelength was used to ensure that only visible light above 420 nm reached the samples, effectively blocking shorter wavelengths during the experiments. Figure 1 presents a schematic illustration of the experimental setup used for testing NO abatement.

To differentiate the intrinsic photocatalytic activity of red mud from the synergistic effects introduced by TiO_2, the NO abatement performances of uncoated red mud mortar and TiO_2-coated red mud mortar are compared. This enables evaluation of whether red mud alone functions as a visible-light photocatalyst for NO removal and whether TiO_2 addition enhances this effect. For TiO_2 coating, a pipette is used to apply two layers of TiO_2 solution (0.01 g TiO_2/mL ethanol, 1.5 mL per layer) onto the red mud-based cement substrate, following the method of [15]. Heat treatment at 300 °C for 1.5 h is employed to immobilize the TiO_2 layer and promote TiO_2–Fe_2O_3 heterojunction formation. In this study, "CO" designates samples with TiO_2 coating only, while "CI" refers to coated samples subjected to immobilization by heat treatment.

Table 1: Chemical composition of cement (CEM III) and red mud (RM-OD and RM-I).

Element oxides %	CEM III	RM-OD	RM-I	Element oxides %	CEM III	RM-OD	RM-I
CaO	58.39	3.44	3.43	MnO	0.13	0.12	0.12
MgO	3.81	0.34	0.44	ZrO_2	0.03	0.34	0.29
Al_2O_3	7.47	16.33	16.1	SrO	0.13	0.02	0.02
SiO_2	21.22	7.01	6.81	TiO_2	0.50	8.30	7.61
Fe_2O_3	2.58	58.94	59.88	V_2O_5	0.03	0.33	0.31
SO_3	4.25	0.49	0.5	Cr_2O_3	0.03	0.32	0.32
K_2O	1.00	0.11	0.07	Sc_2O_3	0.29	-	-
Na_2O	-	3.71	3.94				

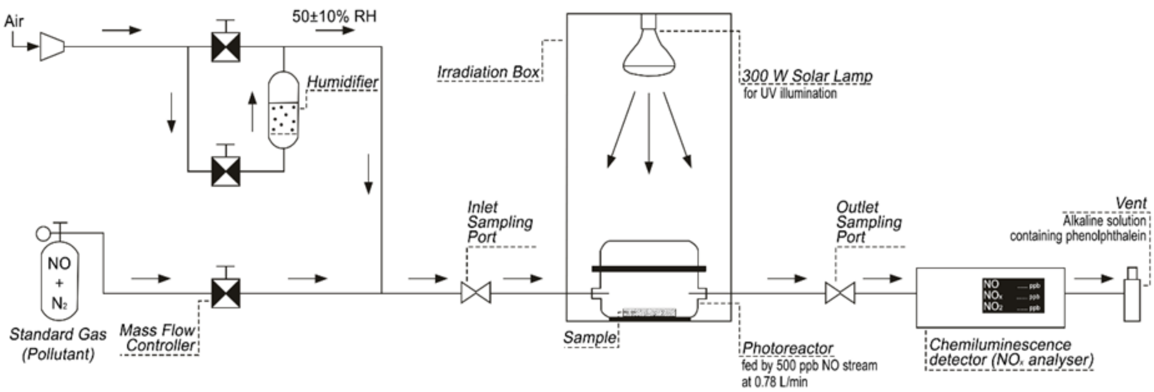

Figure 1: Test setup used for measuring NO and NOx abatement.

3 Results and discussion

3.1 Hydration heat analysis

Figures 2a and 2b display the normalized heat release rate and cumulative heat release for both control and red mud-based cement pastes. During the pre-induction phase, C_3A rapidly reacts with water and sulfates, generating an initial heat peak. The high alkalinity of red mud accelerates C_3A dissolution and ion release, but sulfate ions from gypsum direct the reaction toward sulfoaluminate formation, primarily ettringite.

During the induction (dormancy) period, the reaction and heat release slow down, allowing for workable concrete placement. Tricalcium silicate (C_3S) continues to dissolve, gradually increasing calcium ion concentration. Adding red mud (both RM-OD and RM-I) extends this induction period compared to the control mix, likely due to red mud's high surface area adsorbing calcium ions, which delays key hydration reactions and postpones the acceleration phase. No clear trend is observed between the different types of red mud used.

During cement hydration, the main exothermic peak—driven by rapid C_3S hydration and C-S-H formation—marks the end of the induction period. In red mud (RM)-modified mortars, the acceleration phase is prolonged (8–17 hours) and the main heat peak is reduced, indicating dilution effects and low pozzolanic reactivity. However, incinerated red mud (RM-I) shortens the acceleration period and enhances heat release compared to oven-dried red mud (RM-OD), emphasizing the impact of thermal processing on hydration kinetics.

Following the main hydration peak, a third exothermic peak—associated with tricalcium aluminate (C_3A) hydration and AFm phase formation—emerges as gypsum is depleted. Red mud, rich in alumina and alkalis, intensifies this aluminate peak, particularly in incinerated samples (Figure 2a), resembling the behavior of calcium aluminate cement. Higher red mud content further amplifies and advances this peak, highlighting the influence of red mud composition and processing on cement hydration kinetics.

The steady period follows the deceleration phase, indicating near-equilibrium as most cement hydration reactions conclude and heat evolution stabilizes at a low level. Red mud-based mortars exhibit lower cumulative heat in the first 72 hours compared to the control mix, due to the lower reactivity of red mud and slower early-stage hydration.

The full width at half maximum (FWHM) of the heat flow curve provides valuable information on cement hydration kinetics, reflecting the reaction duration and rate. As shown in Table 2, higher red mud content leads to increased peak heat flow and reduced FWHM, indicating faster, more intense hydration. In contrast, the control and 5% red mud mixes exhibit higher FWHM values, suggesting slower reactions due to limited water diffusion through thicker hydration layers.

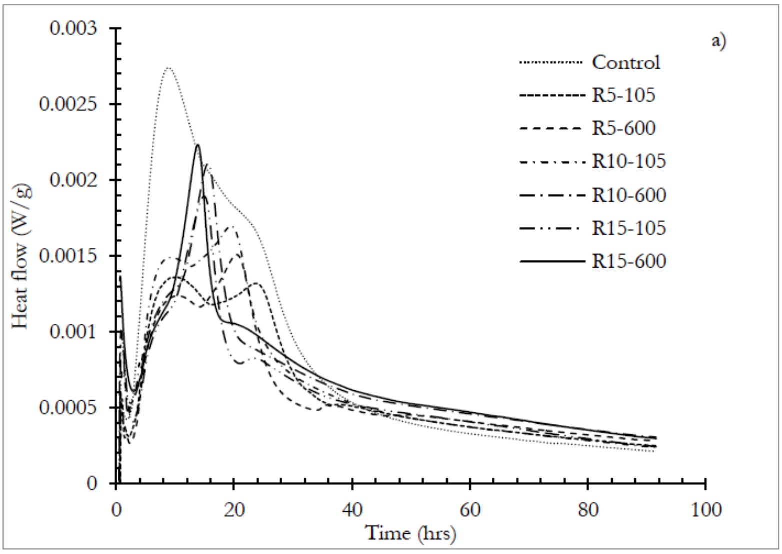

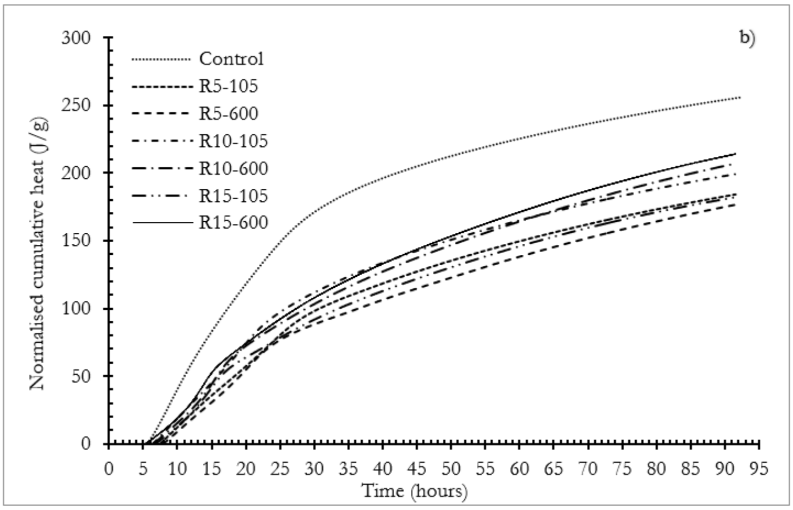

Figure 2: a) Heat release rate and b) cumulative heat release flow curves of mortars.

Table 2: Isothermal calorimetry results of mortars.

Mix	Start of acceleration period	Normalised heat flow at start of acceleration	Arrival time of prominent exothermic peak	Normalised heat flow corresponding to prominent exothermic peak	FWHM value
	hrs:min:sec	mW/g	hrs:min:sec	mW/g	hrs:min
Control	1:49:18	0.42131	8:52:07	273,899	19:30
R5-105	1:27:49	0.30001	10:23:15	135,921	23:00
R10-105	2:29:56	0.52784	19:28:03	169,567	18:00
R15-105	2:47:20	0.40464	14:56:08	189,263	8:30

R5-600	2:19:10	0.26542	10:28:15	123,611	19:00
R10-600	2:14:39	0.46450	15:34:27	210,730	8:30
R15-600	2:54:14	0.60670	13:50:18	223,199	5.30

Typical nomenclature for the investigated mortar mix is represented as RX-Y, where X represents replacement levels of cement with RM (5, 10 or 15), and Y represents the treated temperature (either 105°C or 600°C).

3.2 Mechanical strength – compressive strength and flexural strength

Mortars with 5–10% oven-dried red mud (RM-OD) substitution (R5-105 and R10-105) exhibited comparable 7-day compressive strength to the control mix, while 15% substitution (R15-105) resulted in a 23% strength reduction. In contrast, RM-I mortars (R5-600 and R10-600) showed slight strength gains (3–8%) over the control, though R15-600 remained lower. The high surface area of red mud may enhance initial hydration but reduce water availability, limiting strength development. Overall, RM-I mortars outperformed RM-OD at higher replacement levels due to better interaction with cement hydration products.

At 28 days, the strength trend persisted: higher red mud content resulted in greater strength reduction. R5-105 matched the control (37.38 MPa vs. 37 MPa), while R10-105 and R15-105 showed 20% and 44% decreases, respectively. RM-I mortars exhibited a 17–31% drop compared to the control. Normalizing compressive strength to cement content revealed that red mud, in both oven-dried and incinerated forms, acted primarily as an inert filler and did not significantly contribute to strength development.

The reduced strength is attributed to the dilution of cement and the inert nature of red mud, which contains high iron oxide and lower CaO and SiO_2 than the reference mix. The predominance of inert hematite further limits reactivity and pozzolanic contribution. Overall, red mud's limited reactivity, high alkalinity, and low hydration product formation restrict its effectiveness as a strength-enhancing cement substitute.

Regardless of red mud type, mortars with red mud showed slightly improved 7-day flexural strength compared to the control, with R15-105 matching the control. RM-I based mortars consistently outperformed RM-OD at all levels, likely due to enhanced early hydration. At 28 days, 5–10% red mud replacements maintained flexural strength comparable to the control, while higher levels (R15-105 and R15-600) showed 11–18% reductions.

Table 3: Engineering properties of investigated mortars.

Sample ID	**Compressive strength**		**Flexural strength**		**Pore size distribution**			
	7-day	28-day	7-day	28-day	<20	20-50	50-200	>200
	MPa	MPa	MPa	MPa	nm	nm	nm	nm

Control	21.56	37.00	6.59	7.40	66.91	11.05	6.14	15.89
R5-105	22.41 (23.59)*	37.38 (39.35)*	7.25	7.25	44.08	19.72	10.18	26.02
R10-105	20.30 (22.56)*	29.80 (33.11)*	6.80	7.20	34.77	21.48	15.87	27.87
R15-105	16.54 (19.46)*	20.59 (24.22)*	6.54	6.10	28.87	27.41	22.81	20.90
R5-600	22.19 (23.36)*	29.94 (32.01)*	6.93	7.96	53.03	16.27	8.72	21.99
R10-600	23.33 (25.92)*	29.70 (33.48)*	7.4	7.73	50.39	14.51	13.80	21.30
R15-600	19.90 (23.41)*	25.41 (30.47)*	7.31	6.57	43.63	16.73	15.82	23.82

**Values in parentheses indicate the normalised compressive strength.*

3.3 Porosity

The open porosity and pore size distribution of the mortars were evaluated using Mercury Intrusion Porosimetry (MIP). Pores were classified as harmless (<20 nm), less-harmful (20–50 nm), harmful (50–200 nm), and more harmful (>200 nm). Incorporation of red mud increased overall porosity and shifted the pore size distribution towards a higher proportion of larger pores (50–200 nm and >200 nm), as shown in Table 3. This is attributed to the lower CaO and SiO_2 content in red mud, which limits strength development and pore refinement, resulting in a more porous microstructure.

Mortars with RM-OD exhibited a greater fraction of large pores compared to those with RM-I, consistent with previous findings that red mud addition increases porosity and water absorption while reducing compressive strength [17]. At 5% and 10% replacement levels, red mud led to more fine pores and fewer large pores, but at 15%, there was a significant increase in connected larger pores, further reducing compressive strength. These results confirm the direct relationship between pore structure and mechanical performance in red mud-modified mortars.

3.4 NO abatement test

The photocatalytic efficiency of red mud-modified mortars for NO removal was assessed under solar and visible light, following UNE 127197-1 [18] standard. All tested samples achieved Class 3 performance (>8% NO degradation), indicating strong air purification capability. Key factors contributing to this activity include high surface alkalinity, porosity, and roughness, which promote radical formation and mass transfer. Mortars with oven-dried red mud (RM-OD) exhibited a higher proportion of large pores (≥50 nm), enhancing reactant accessibility and overall photocatalytic performance.

Under visible light, the R5-105-F-CI sample exhibited significantly enhanced photocatalytic activity, with 26% and 49% higher NO and NO_x removal, respectively, compared to R5-105-F-CO. This improvement is attributed to the synergistic interaction between Fe_2O_3 and TiO_2, enhanced by heat treatment, which promotes efficient charge separation and transfer at the Fe_2O_3/TiO_2 interface, thereby reducing recombination and increasing pollutant degradation efficiency.

The proposed technology demonstrates significant promise for advanced environmental remediation, particularly in facilitating efficient air purification and enabling the degradation of hazardous organic compounds within indoor environments. It is particularly suited for non-structural applications, such as red mud-based tiles, where high compressive strength is not a primary requirement.

Table 4: Percentage abatement of NO and NOx of RM-based mortars under solar irradiation and visible light.

Sample ID	**NO**	**NOx**
	%	%
R5-105	10.2	10.6
R5-105-F	9.4	9.2
R10-105	17.1	16.5
R10-105-F	14.3	14
R15-105	20.4	18.9
R15-105-F	14	13.7
R5-600	9.1	8.4
R5-600-F	9.7	9.6
R10-600	15.8	14.1
R10-600-F	10.2	9.1
R15-600	14.5	13.8
R15-600-F	8.1	7.3
R5-105-CO	73.1	44.9
R5-105-CO-F	45.8	32.4
R5-105-CI	71.7	62.0
R5-105-CI-F	57.8	48.2

Samples with abbreviations ending in 'F' indicate that these were tested under strict visible light conditions.

G. Kaur, J. M. Fernández, I. Navarro-Blasco, S. Pavia, J I Álvarez (2025) From Toxic Waste to Sustainable Building: Red mud Cementitious Composites for Environmental Remediation
Proceedings ICSBM 2025 : 4th International Conference on Sustainable Building Materials: Volume 4 : Traditional and New Cementitious Materials ISBN 978-90-386-6618-1
----

4 Conclusions

1 The addition of red mud in mortar leads to a reduction in compressive strength primarily due to the dilution of cement and the inert nature of red mud. While red mud may marginally improve particle packing as a filler. However, the limited ability of red mud to generate hydration products significantly hinder its contribution to strength development in mortar mixes.

2 Calcination at 600°C does not significantly affect the pozzolanic activity of the red mud sample examined in this study. Although improvement in the compressive strength of red mud-based mortars at higher replacements is minimal; yet mortars containing 5% red mud performed similar as that of control mix.

3 Red mud increases overall porosity with respect to control mix by shifting the pore size distribution toward more pores ≥50 nm.

4 Incorporating red mud into cementitious mortars produces materials with strong photocatalytic NO and NOx removal efficiency (Class 3, >8% NO degradation) making these mortars promising for air purification and sustainable construction applications.

5 The superior photocatalytic activity of the TiO_2-coated sample (R5-105-CI) under solar and visible light is attributed to the synergistic effect between Fe_2O_3 and TiO_2, which extends light absorption into the visible range and results in 26% and 49% higher abatement of NO and NOx, respectively.

Acknowledgments

This research was funded by the European Union's Horizon 2020 research and innovation programme under the Marie Skłodowska-Curie grant agreement No 101034345 and the Ministerio de Ciencia e Innovación, grant number TED2021-129705B-C33 Terra-Cycle by MICINN/AEI/10.13039/501100011033.

References

1. Xiao Liu, Yuexin Han, Fayu He, Peng Gao, Shuai Yuan, Characteristic, hazard and iron recovery technology of red mud - A critical review, Journal of Hazardous Materials, Volume 420, 2021, 126542, ISSN 0304-3894, https://doi.org/10.1016/j.jhazmat.2021.126542.

2. Peixin Du, Peng Wang, Xueqian Zhang, Guangwu Wen, Yishan Wang, Properties, hazards and valuable metal recovery technologies of red mud: A review, Particuology, Volume 93, 2024, Pages 328-348, ISSN 1674-2001, https://doi.org/10.1016/j.partic.2024.07.010.

3. International Aluminium Institute. International aluminium institute launches bauxite residue roadmap [Internet]. 2024 [cited 2025 May 5]. Available from: https://international-aluminium.org/news-recycling/

4. Adela Svobodova-Sedlackova, Alejandro Calderón, Inés Fernandez, Josep Maria Chimenos, Carlos Berlanga, Onuralp Yücel, Camila Barreneche, Rafael Rodriguez, Mapping the research landscape of bauxite by-products (red mud): An evolutionary perspective from 1995 to 2022, Heliyon, Volume 10, 2024, e24943, ISSN 2405-8440, https://doi.org/10.1016/j.heliyon.2024.e24943.

5. Jizhe Zhang, Shengjie Liu, Zhanyong Yao, Shaopeng Wu, Hongguang Jiang, Ming Liang, Yaning Qiao, Environmental aspects and pavement properties of red mud waste as the replacement of mineral filler in asphalt mixture, Construction and Building Materials, Volume 180, 2018, Pages 605-613, ISSN 0950-0618, https://doi.org/10.1016/j.conbuildmat.2018.05.268.

6. Aman Kumar, Jothi Saravanan, Kunal Bisht, Syed Ahmed Kabeer, A review on the utilization of red mud for the production of geopolymer and alkali activated concrete, Construction and Building Materials, Volume 302, 2021, 124170, ISSN 0950-0618, https://doi.org/10.1016/j.conbuildmat.2021.124170.

7. Khanna, Rita, Yuri Konyukhov, Dmitry Zinoveev, Kalidoss Jayasankar, Igor Burmistrov, Maksim Kravchenko, and Partha S. Mukherjee. 2022. Red Mud as a Secondary Resource of Low-Grade Iron: A Global Perspective, Sustainability, Volume 14, 1258. https://doi.org/10.3390/su14031258.

8. Vikash Singh, Samreen Bano, Vinay Bhushan Chauhan, Priyaranjan Pal, Anil Kumar, Jyoti Bhushan Srivastava, Red mud as a sustainable road construction material: An experimental investigation, Construction and Building Materials, Volume 411, 2024, 134549, ISSN 0950-0618, https://doi.org/10.1016/j.conbuildmat.2023.134549.

9. Dan Zhao, Yang Ma, Jinguang Zhao, Heng Chen, Qinfei Li, João Castro Gomes, Hervé Kouamo Tchakouté, Xin Cheng, Pengkun Hou, Effect of thermal activation on the physicochemical property evolution of red mud and its application in low-carbon binder preparation, Journal of Building Engineering, Volume 104, 2025, 112376, ISSN 2352-7102, https://doi.org/10.1016/j.jobe.2025.112376.

10. Eliz Paula Manfroi, Malik Cheriaf, Janaíde Cavalcante Rocha, Microstructure, mineralogy and environmental evaluation of cementitious composites produced with red mud waste, Construction and Building Materials, Volume 67, 2014, Pages 29-36, ISSN 0950-0618, https://doi.org/10.1016/j.conbuildmat.2013.10.031.

11. Shaoliang Chen, Abdul Ghani Razaqpur, Tuanjie Wang, Effects of a red mud mineralogical composition versus calcination on its pozzolanicity, Construction and Building Materials, Volume 404, 2023, 133238, ISSN 0950-0618, https://doi.org/10.1016/j.conbuildmat.2023.133238.

12. Manoj Kumar Sahu and Raj Kishore Patel, Novel visible-light-driven cobalt loaded neutralized red mud (Co/NRM) composite with photocatalytic activity toward methylene blue dye degradation, Journal of Industrial and Engineering Chemistry, Volume 40, 2016, Pages 72-82, ISSN 1226-086X, https://doi.org/10.1016/j.jiec.2016.06.008.

13. Jinshan Tang, Zhiliang Cheng, Qian Xu, Jinyu Sun, Fangyi Li, Facheng Qiu, Bagasse modification of red mud for efficient photocatalytic degradation of real dye wastewater: An utilization attempt for massive waste, Environmental Research, Volume 267, 2025, 120608, ISSN 0013-9351, https://doi.org/10.1016/j.envres.2024.120608.

14. Mahdieh Chegeni, Mozhgan Mehri, Sara Dehdashtian, Photocatalytic bauxite and red mud/graphitic carbon nitride composites for Rhodamine B removal, Journal of Molecular Structure, Volume 1242, 2021, 130752, ISSN 0022-2860, https://doi.org/10.1016/j.molstruc.2021.130752.

15. Marianne Smits, Chun kit Chan, Tom Tytgat, Bart Craeye, Nathalie Costarramone, Sylvie Lacombe, Silvia Lenaerts, Photocatalytic degradation of soot deposition: Self-cleaning effect on titanium dioxide coated cementitious materials, Chemical Engineering Journal, Volume 222, 2013, Pages 411-418, ISSN 1385-8947, https://doi.org/10.1016/j.cej.2013.02.089.

16. Linlin Peng, Tengfeng Xie, Yongchun Lu, Haimei Fan and Dejun Wang, Synthesis, photoelectric properties and photocatalytic activity of the Fe2O3/TiO2 heterogeneous photocatalysts, Physical Chemistry Chemical Physics, 2010,12, 8033-8041, DOI https://doi.org/10.1039/C002460K.

17. Jing Shu, Dewen Kong, Lingling Wang, Nauman Khan, Shenghui Zhou, Yurui Han, Tiejun Tao, Tao Zheng, Performance and microstructure of red-mud-blended concrete under different aqueous environments, Construction and Building Materials, Volume 447, 2024, 137988, ISSN 0950-0618, https://doi.org/10.1016/j.conbuildmat.2024.137988.

18. UNE 127197-1:2013, Test Method Application to Evaluate the Air-Purification Performance of Semiconducting Photocatalytic Materials Soaked into Precast Concrete Products – Part 1: Removal of Nitric Oxide, Spanish Association for Standardization (UNE), Madrid, 2013.